Three-body recombination rate of atomic nitrogen in low pressure plasma flows

A. Bourdon, Pierre Vervisch

Three-body recombination rate of atomic nitrogen in low-pressure plasma flows

A. Bourdon* and P. Vervisch
Université de Rouen, CNRS URA 230 CORIA, 76821 Mont Saint Aignan Cedex, France
(Received 11 March 1996)

A nonlinear collisional-radiative model for atomic nitrogen has been developed in order to determine effective recombination and associated ionization coefficients for either optically thin or optically thick plasmas where 10^{18} m$^{-3} \leqslant n_e \leqslant 10^{21}$ m^{-3} and 2000 K$\leqslant T_e \leqslant$12 000 K. A time-dependent approach confirms the importance of the quasi-steady-state condition to derive meaningful rate coefficients. In order to implement these coefficients in plasma flow codes, simple analytical expressions are proposed. Significant discrepancies with existing literature values are pointed out and discussed. In recombining conditions, the relaxation time necessary to reach the quasi-steady-state is calculated, and depends on the electron number density and on the electron temperature. This time limits the validity of the recombination coefficient, especially in optically thick cases. Finally, for practical applications, the number of levels in Saha-Boltzmann equilibrium at the quasi-steady-state is also examined. [S1063-651X(96)09908-4]

PACS number(s): 52.25.Jm, 34.10.+x

I. INTRODUCTION

The experimental determination of the effective three-body recombination rate remains a difficult issue; therefore most available results have been derived from theoretical studies. However, the effective recombination reaction $N^+ + 2e^- \rightarrow N + e^-$ results from numerous different elementary processes between the atomic levels of nitrogen. Hence the accuracy of theoretical three-body recombination rates depends on the choice of the atomic model and of the rate coefficients for the elementary processes.

In earlier models for nitrogen [1–4], more or less sophisticated atomic models were considered, and the elementary rate coefficients used were those initially derived for hydrogen and only slightly modified to adapt to nitrogen. Nevertheless, the theoretical three-body recombination rate determined by Park [1] for an optically thick medium was in agreement with the main experimental data [5], which are limited to a small range of plasma parameters ($n_e \approx 10^{21}$ m^{-3} and $T_e \approx 10\,000$ K, where n_e is the electron number density and T_e is the electron temperature). In fact, usually in the computation of plasma flows, whatever the importance of radiative processes and the electron temperature range in the medium, the very simple analytical form proposed by Park [1] for 4000 K$\leqslant T_e \leqslant$20 000 K is implemented.

In this paper, we propose to set up a time-dependent nonequilibrium collisional-radiative model for atomic nitrogen in order to determine the effective three-body recombination rate (denoted k_r) for 10^{18} m$^{-3} \leqslant n_e \leqslant 10^{21}$ m^{-3} and 2000 K$\leqslant T_e \leqslant$12 000 K. Earlier studies have been carried out for $T_e \geqslant$4000 K, but we also focus on lower electron temperatures which may be met in supersonic or hypersonic flows in high enthalpy wind tunnels and especially at the vicinity of blunt bodies. In this work, we consider a spatially uniform and electrically neutral plasma, and assume that the distributions of energies of particles are Maxwellian.

We use the elementary rate coefficients critically compiled by Kunc and Soon [6] in their study on the radiation emitted by a nonequilibrium stationary atomic nitrogen plasma. We update their data on e-N inelastic collisions [7] and on Einstein coefficients [8–10].

The interest of a time-dependent approach is the possibility to follow the temporal relaxation of atomic level populations and then to study in nitrogen the validity of the quasi-steady-state hypothesis, already discussed in other plasmas (in hydrogen [11,12], helium [13], and oxygen [14]). We also determine the location of the lowest atomic level whose population is in Saha-Boltzmann equilibrium. This level, usually called the critical level [15], is useful for experimental studies since it indicates that lowest level whereby spectral intensity measurements can be used to ascertain the kinetic temperature of the free-electron distribution. All these results are discussed, and applied to the study of low-pressure supersonic recombining nitrogen plasma flows. The treatment of radiation is limited to either optically thick or optically thin cases.

II. ATOMIC MODEL

In the electron temperature range of our study, we consider only the ground term of N^+, $2s^2 2p^2\ ^3P$ (14.54 eV) which is taken as the ''core'' for all atoms. In atomic nitrogen, there is a large energy gap between the two metastable levels ($2s^2 2p^3\ ^2D^0$ and $2s^2 2p^3\ ^2P^0$) with low excitation energies (2.38 and 3.58 eV respectively), and the resonant level which excitation energy is about 10 eV. As a result, most of the excited levels lie in a narrow region of energy, and are usually coalesced in a reduced number of levels. However, this procedure is somewhat arbitrary when the density of levels is high, and therefore different atomic models exist for nitrogen. For highly excited levels, one should also take into account the ionization potential lowering. Indeed, the ionization energy and thus the number of bound atomic levels of an atom in a plasma are generally smaller than those of an isolated atom. Two different theoretical approaches exist to estimate the ionization potential lowering ΔE. First, considering the influence of all the charged species surrounding the

*Electronic address: Anne.Bourdon@coria.fr

TABLE I. Comparisons of different atomic models in nitrogen. np is the total number of atomic levels and $E(np)$ is the energy of the last bound level.

Atomic models	np	$E(np)$ (eV)	T_e range (10^3 K)	n_e range (m^{-3})
Kulander [2]	5	11.80	10–1000	10^{24}–10^{27}
Park [18]	41	14.47	$\geqslant 8$	$\geqslant 10^{20}$
Park [19]	35	14.49	4–11	10^{19}–10^{22}
Potapov *et al.* [3]	63	14.35	4–20	10^{16}–10^{24}
Taylor and Ali [4]	13	12.82	11–30	10^{22}–10^{25}
Kunc and Soon [6]	14	12.92	8–15	
Park [20]	22	14.41		
Our model	43	14.47	2–12	10^{18}–10^{21}

atom in the plasma, Griem [15] proposed (Debye shielding)

$$\Delta E = 2.95\times 10^{-11}\left(\frac{n_e}{T_e}\right)^{1/2} \text{ eV}. \tag{1}$$

Second, considering only the influence of the closest ion on the atom, Unsöld [16] obtained a value of ΔE which exceeds the one given by Griem by up to a factor of 4. Some authors simply sum both contributions to obtain the true ionization potential lowering. However, Olsen [17] showed that the Debye shielding formula should be used in plasmas where the electron number density is lower than 10^{25} m^{-3}. Therefore in our conditions, we can estimate the maximal ionization potential lowering by

$$\Delta E_{\max} = 2.95\times 10^{-11}\left(\frac{[n_e]_{\max}}{[T_e]_{\min}}\right)^{1/2} \approx 0.02 \text{ eV}. \tag{2}$$

This very small value indicates that, within our temperature and density ranges, the ionization potential lowering is negligible and the maximum number of atomic levels has to be taken into account. Table I compares the number of atomic levels considered in different studies on nitrogen. It clearly appears that the 14 level atomic model proposed by Kunc and Soon [6], in which the last bound level lies 1.62 eV under the ionization potential, does not meet the condition of Eq. (2).

However, in order to use the elementary rate coefficients reviewed by Kunc and Soon, we have tried to find an atomic model close to their model for the excited levels, the energy of which is less than or equal to 12.92 eV. Among the different atomic models for nitrogen given in Table I, the 41-level model proposed by Park [18] appears to be the closest if we split the group of states labeled 10 and 13. It is interesting to note that the group of states labeled 12 in Park's model has not been considered by Kunc and Soon, even though this group of states generates the intense 1243 Å lines.

Finally, in this paper, we take into account a 43-atomic-level model in which the last bound level lies only at 0.07 eV from the continuum. We will show in the following sections that, in our conditions, this atomic model turns out to be a good compromise between the negligible ionization potential lowering and the inaccuracy of atomic models for highly excited levels.

III. ELEMENTARY RATE COEFFICIENTS

In a uniform plasma, the evolution of the population density of an excited atomic level i is due to different elementary processes. We neglect atom-atom and atom-ion inelastic collisions in comparison to the electron-atom collisions, and retain

$$N_i + e^- \underset{C_{ji}}{\overset{C_{ij}}{\rightleftarrows}} N_j + e^- \quad \text{for } i<j, \tag{3}$$

where C_{ij} ($m^3\,s^{-1}$) and C_{ji} ($m^3\,s^{-1}$) are, respectively, the electron-impact excitation rate coefficient for the transition from the level i to the level j and its inverse deexcitation rate coefficient

$$N_i + e^- \underset{\beta_{ci}}{\overset{\beta_{ic}}{\rightleftarrows}} N^+ + 2e^-, \tag{4}$$

where β_{ic} ($m^3\,s^{-1}$) and β_{ci} ($m^6\,s^{-1}$) are, respectively, the electron-impact ionization rate coefficient from the level i and the three-body recombination rate coefficient on the level i;

$$N_j \xrightarrow{A_{ji}} N_i + h\nu \quad \text{for } i<j, \tag{5}$$

where A_{ji} (s^{-1}) is the transition probability (Einstein coefficient) from the level j to the level i; and

$$N^+ + e^- \xrightarrow{\alpha_i^{\mathrm{RR}} + \alpha_i^{\mathrm{RD}}} N_i + e^-, \tag{6}$$

where α_i^{RR} ($m^3\,s^{-1}$) and α_i^{RD} ($m^3\,s^{-1}$) are, respectively, the radiative and dielectronic recombination rate coefficients on the level i. Dielectronic recombination is in fact the result of a two-stage process [6]:

$$N^+ + e^- \rightarrow N^* \rightarrow N_i + h\nu, \tag{7}$$

where N^* represents an autoionizing state of the N atom.

A. Electron-impact excitation and deexcitation rate coefficients

Experimental data being very scarce, excitation cross sections are determined theoretically. We use the formalism developed by Sobelman, Vainshtein, and Yukov [21] for all transitions between the lowest atomic levels, the energy of which is less than or equal to 12.92 eV. ''Difficult'' transitions (i.e., involving two atomic electrons) turned out to have a negligible influence in our conditions and the associated rates are derived from a binary-encounter approximation. All details are given in the paper of Kunc and Soon [6]. For atomic levels close to the continuum, all atoms are almost hydrogenic. Therefore, the formalism initially developed for hydrogen by Gryzinski [22] is used for these levels, and is no doubt more adapted than the Vainshtein formalism.

The use of two different theoretical approaches results in abrupt changes in the rate coefficient values for intermediate transitions (namely, $10<i<20 \leftrightarrow i-5<j<i+5$). In order to eliminate this anomaly already mentioned in other plasma studies [23], we introduce, in the same way, a correction factor such that rate coefficient values vary smoothly from

one model to the other. Discrepancies on the effective three-body recombination rate coefficient k_r values due to this correction remain within a factor of 2.

For transitions between the three lowest atomic levels (ground state and the metastables), excitation cross sections calculated recently by Ramsbottom and Bell [7] have been used. These results seem to be much more accurate than those determined earlier by Henry, Burke, and Sinfailam [24], and used by Kunc and Soon.

B. Electron-impact ionization and three-body recombination rate coefficients

For the ground state and the two lowest excited levels, the models retained by Kunc and Soon have been used. For the other atomic levels, the good agreement noted between the rate coefficient values given by different hydrogenic models [21,25,26] led us to use the classical model approximation derived by Gryzinski and Kunc [26].

C. Spontaneous emission

Electric dipole transition probabilities being far much higher than those of electric quadripole and magnetic dipole transitions, the latter have been neglected. For excited levels, the energy of which is less than or equal to 12.92 eV, we have taken into account all the transitions reviewed by Kunc and Soon and added the 1243 Å lines. We have also considered transitions issuing from atomic levels lying higher than 12.92 eV. For all transitions, the best possible Einstein coefficients available in the literature have been used [6,8,9,10,27,28]. However, the higher the principal quantum number of an atomic level, the less efficient the radiative processes are in comparison to collisions. Thus, in our model, all atomic levels lying higher than 13.7 eV have been considered as nonradiative levels.

D. Radiative and dielectronic recombinations

Nussbaumer and Storey [29,30] showed that the two-stage process of dielectronic recombination is much more efficient than the radiative recombination process at electron temperatures below 20 000 K. For both recombination processes, we consider only the coefficients for the effective (direct plus cascade) transitions to the three first atomic levels. For dielectronic recombination, the effective recombination rate coefficient α_i^{RD} for $i=1$, 2, and 3 has been fitted by Nussbaumer and Storey, and finally the total dielectronic recombination rate is

$$\alpha^{\mathrm{RD}}=\sum_{i=1}^{3}\alpha_i^{\mathrm{RD}}=1\times10^{-12}[0.631+0.2\times10^{-4}T_e]T_e^{-1.5}\times\exp\left(\frac{-4398}{T_e}\right)\ \mathrm{m^3\,s^{-1}}. \tag{8}$$

The radiative recombination cross sections have been derived from the photoionization cross sections determined by Henry [31]. We have calculated and fitted the associated total radiative recombination rate, and obtained

$$\alpha^{\mathrm{RR}}=\sum_{i=1}^{3}\alpha_i^{\mathrm{RR}}=7.64\times10^{-18}T_e^{-0.4}\ \mathrm{m^3\,s^{-1}}. \tag{9}$$

IV. MASTER EQUATIONS

As a result of the different elementary processes mentioned above, the rate equation describing the evolution of the population density denoted N_i ($\mathrm{m^{-3}}$) of the atomic level labeled i can be written as

$$\frac{dN_i}{dt}=\dot{N}_i=\sum_{j\neq i}n_eN_jC_{ji}+\sum_{j>i}N_jA_{ji}\kappa_{ji}+n_eN^+\times[\alpha_i^{\mathrm{RR}}\kappa_i^{\mathrm{RR}}+\alpha_i^{\mathrm{RD}}\kappa_i^{\mathrm{RD}}+n_e\beta_{ci}]-N_i\left[\sum_{j\neq i}n_eC_{ij}+\sum_{k<i}A_{ik}\kappa_{ik}+n_e\beta_{ic}\right]. \tag{10}$$

for $1\leqslant i\leqslant np$, where np is the total number of atomic levels, n_e ($\mathrm{m^{-3}}$) the electron number density and N^+ ($\mathrm{m^{-3}}$) the number density of $\mathrm{N^+}$. For the escape factors denoted κ_{ij}, κ_i^{RR} and κ_i^{RD}, respectively, for bound-bound, free-bound, and dielectronic radiation, we consider only the limit cases where they are equal either to 0 (optically thick plasma) or to 1 (optically thin plasma).

The rate equation for the production of electrons is

$$\frac{dn_e}{dt}=\dot{n}_e=\sum_i n_eN_i\beta_{ic}-\sum_i n_e^2N^+\beta_{ci}-\sum_i n_eN^+[\alpha_i^{\mathrm{RR}}\kappa_i^{\mathrm{RR}}+\alpha_i^{\mathrm{RD}}\kappa_i^{\mathrm{RD}}]. \tag{11}$$

Finally, the electrical neutrality of the plasma imposes $n_e=N^+$. We note that $N_a=\Sigma N_i$, the total atomic density and $N_t=N_a+N^+$, the total particle density.

The system of differential equations [Eqs. (10) and (11)] has been integrated numerically in using LSODE [32], a routine specifically designed to solve stiff ordinary differential equations. In each set of calculations, we keep T_e and the total particle density N_t constant.

V. RESULTS AND DISCUSSION

A. General behavior of time-dependent population densities

Figures 1(a) and 1(b) show the temporal evolution of the level populations for an initial recombining situation at $t=0$ s: $n_e=10^{20}$ $\mathrm{m^{-3}}$, $T_e=8000$ K, and $N_a=10^{18}$ $\mathrm{m^{-3}}$, and all atomic levels are assumed to be in Boltzmann equilibrium with the ground state at the electron temperature T_e. All elementary processes described above are taken into account, and the plasma is considered to be optically thin. This initial condition represents the temperature and densities measured in a particular low-pressure nitrogen plasma flow [33]. However, it is important to point out that the general characteristics of the time-dependent results do not depend on the choice of the initial recombining condition.

In early times, the variations of N_1, N_2, N_3, and n_e are negligible, whereas the other excited level populations increase and reach a plateau (at $t\approx3\times10^{-8}$ s and until $t\approx10^{-5}$ s, in this example). It is interesting to note that the excited

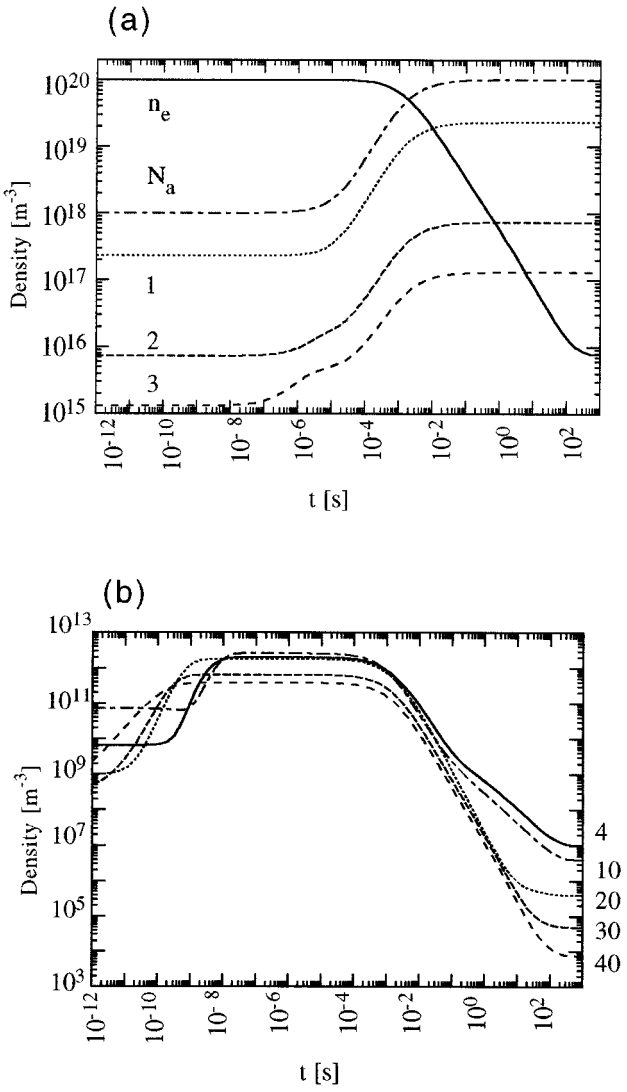

FIG. 1. (a) and (b) Temporal evolution of densities for an initial recombining situation: T_e=8000 K, $n_e=10^{20}$ m^{-3}, and $N_a=10^{18}$ m^{-3}, and considering all atomic levels in Boltzmann equilibrium with the atomic ground state at T_e. All elementary processes are taken into account, and the plasma is considered to be optically thin. Numbers denote atomic level numbers. Atomic level population densities have been divided by their statistical weights.

level populations at the plateau are very different from those corresponding to the stationary state of the system (reached in this example after 10^3 s). In fact, this plateau corresponds to the stationary state of the excited level ($i>3$) populations with the initial values of T_e, n_e, N_1, N_2, and N_3. Figures 1(a) and 1(b) clearly illustrate on a particular situation that very different time scales characterize the global relaxation process. Figure 2 shows the temporal evolutions of $|\dot{n}_e|$ and N_i for $1\leqslant i\leqslant 3$. We note that a quasi-steady-state condition of the form

$$|\dot{n}_e|=\dot{N}_1+\dot{N}_2+\dot{N}_3 \tag{12}$$

is satisfied for $t\geqslant\tau_{\min}$ ($\tau_{\min}=3\times10^{-8}$ s in this example).

For hydrogen, the corresponding quasi-steady-state (QSS) condition [34] takes into account only the ground state of the

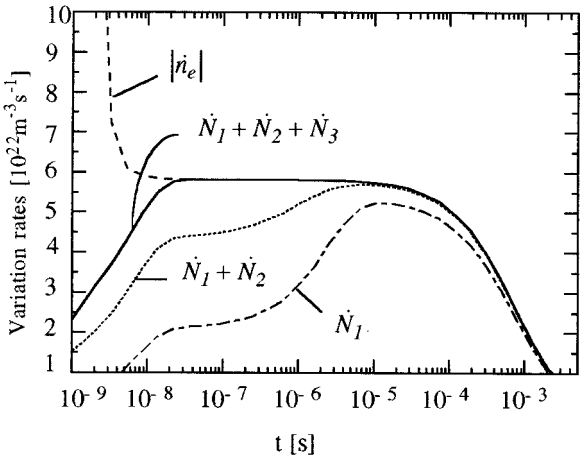

FIG. 2. Production rates of N_1, N_2, and N_3, and the depletion rate of n_e for the same initial recombining condition as in Fig. 1.

atom. For nitrogen, Fig. 2 clearly shows the necessity to consider also the contribution of the two metastable levels. In fact, most earlier collisional-radiative models have been developed with less powerful numerical tools than the one used in this paper. Therefore, in his study [1], Park assumed that Eq. (12) was the QSS condition in nitrogen, in order to simplify his calculations. In this work, this condition appears freely during the temporal relaxation.

B. General method to determine the effective three-body recombination rate coefficient

For the global reaction $N^+ + 2e^- \leftrightarrow N + e^-$, we define k_r, the effective three-body recombination rate coefficient, and k_i, the effective ionization rate coefficient, such that

$$\frac{dn_e}{dt}=\dot{n}_e=k_i n_e N_a - k_r n_e^3. \tag{13}$$

Both rate coefficients have to be time independent, but may depend on electron temperature and densities. Starting at $t=0$ s, from a recombining situation, in early times, the first term of Eq. (13) is far much smaller than the second one. Therefore, if k_r exists, then the ratio $|\dot{n}_e|/n_e^3$ is constant.

For the initial condition of the last section, Fig. 3 shows that a value of k_r can be determined for $\tau_{\min}\leqslant t\leqslant\tau_{\max}$, with $\tau_{\max}=10^{-5}$ s. The minimal time required corresponds to the relaxation time necessary to reach a quasi-steady-state (Figs. 2 and 3) and is denoted $\tau_{\rm QSS}$ in the following. Then, with no preliminary hypothesis, the present work confirms that a quasi-steady-state has to be reached in order to determine k_r. For $t>\tau_{\max}$, ionization processes become significant, and the first term in Eq. (13) is no longer negligible in comparison to the second one.

In order to determine k_r, first we select an initial recombining condition, and, second, we allow the transient solution to develop until $|\dot{n}_e|$ and $\dot{N}_1+\dot{N}_2+\dot{N}_3$ agree to within 1%. Then we determine $\tau_{\rm QSS}$ and calculate k_r with the instantaneous values of $|\dot{n}_e|$ and n_e^3. The interest of this approach is the possibility to follow the temporal evolutions of population densities and to determine $\tau_{\rm QSS}$.

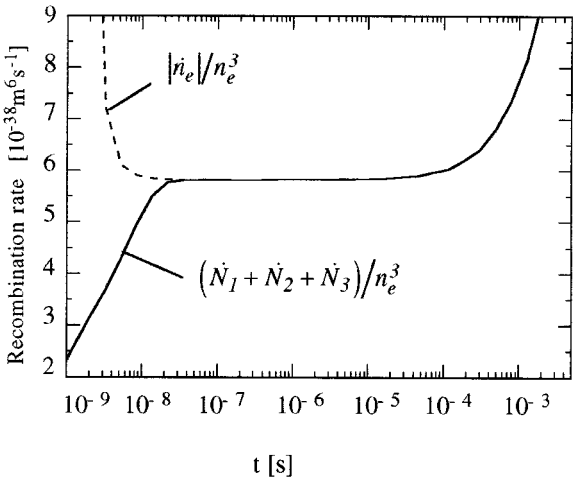

FIG. 3. Time variations of $|\dot{n}_e|/n_e^3$ and $(\dot{N}_1+\dot{N}_2+\dot{N}_3)/n_e^3$ for the same initial recombining condition as in Fig. 1.

C. Optically thick plasma

In order to represent an optically thick medium, all radiative processes have been neglected in this section. As only elementary collisional processes are considered, the obtained results are denoted with the superscript C. It is interesting to note that these results may be applied also to optically thin media where the electron number density is high enough to neglect radiative processes in comparison to collisions.

1. Determination of the effective three-body recombination rate coefficient

After having considered different initial conditions, we have pointed out that in an optically thick medium, the effective three-body recombination rate coefficient k_r^C depends only on the electron temperature, in agreement with earlier studies [1,3]. We have noted no influence of either densities or the initial distribution on the atomic levels. Figure 4 compares the value of k_r^C, determined with our model, with the one given by the fitting law proposed by Park [1]:

$$k_r^C = 1.15\times 10^{-38}\left(\frac{T_e}{10^4}\right)^{-5.27} \quad \mathrm{m^6\,s^{-1}}$$

$$\text{for } 4000\ \mathrm{K} \leqslant T_e \leqslant 20\,000\ \mathrm{K}. \quad (14)$$

Over the whole temperature range, the value obtained with our model remains smaller than the one given by Park's fitting law. The discrepancy between the two rates increases with temperature, and exceeds one order of magnitude for $T_e > 8000$ K. The simplest best-fit curve for our computed results is

$$k_r^C = 1.96\times 10^{-39}\left(\frac{T_e}{10^4}\right)^{-6.04} \quad \mathrm{m^6\,s^{-1}}$$

$$\text{for } 2000\ \mathrm{K} \leqslant T_e \leqslant 12\,000\ \mathrm{K}. \quad (15)$$

With our approach, we have also calculated the effective three-body recombination rate coefficient k_r^C associated with the cross sections derived by Gryzinski [22] for hydrogen, and slightly modified by Park to study nitrogen [1]. That is, nonhydrogenic effects are considered by multiplying the Gryzinski value for the ground state by a factor 3, and for the two metastable levels by a factor 1.5. The corresponding elementary collisional rate coefficient values are close to those used in our model for highly excited levels, but are much higher for low-energy levels. In this case, Fig. 4 shows that the derived effective three-body recombination rate coefficient value is very close to the one given by Park's fitting law even for $2000\ \mathrm{K} \leqslant T_e \leqslant 4000$ K, a temperature range where the validity of this analytical law is uncertain.

At low electron temperature, the good agreement depicted in Fig. 4 between the values of the different effective recombination rates seems to indicate that, for this temperature range, the three-body recombination rate depends greatly on inelastic collisions involving highly excited levels. Conversely, at high electron temperature, the significant discrepancies observed seem to indicate that the recombination rate depends mainly on elementary processes involving low-energy levels.

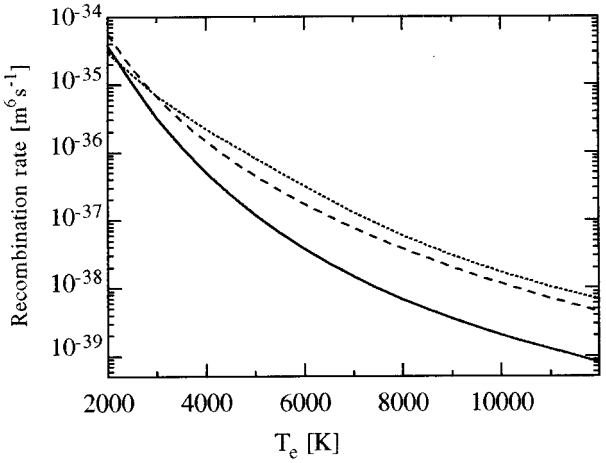

FIG. 4. Three-body recombination rate in an optically thick plasma. Solid line: our model. Dotted line: Park's fitting law [1]. Dashed line: our atomic model and the cross sections derived by Gryzinski, and slightly modified to adapt nitrogen [1].

2. Influence of the number of atomic levels

Figure 5 shows the influence of the number of atomic levels on the calculated recombination rate coefficient value. It clearly illustrates, that the lower the electron temperature, the more numerous atomic levels are required to determine k_r^C. For $T_e \leqslant 2000$ K, we note a discrepancy between the results obtained with our atomic model (43 levels) and the same model involving only 40 levels. This result seems to indicate that our atomic model is not adapted for this low electron temperature range. It also confirms the strong influence of highly excited levels on the three-body recombination rate value at low electron temperatures. In fact, the theoretical determination of k_r^C at low electron temperatures is generally difficult since, the more numerous highly excited atomic levels are taken into account, the higher the derived recombination rate.

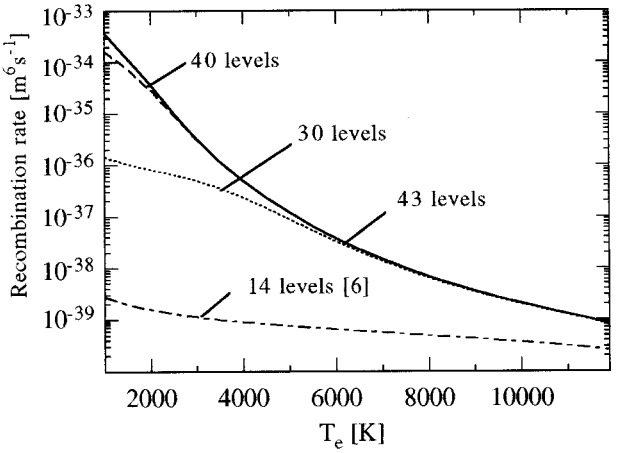

FIG. 5. Influence of the number of atomic levels on the derived recombination rate in an optically thick case.

Finally, Fig. 5 shows that our 43 level atomic model is adapted for studies in the temperature range considered in this study, i.e., 2000 K$\leqslant T_e \leqslant$12 000 K. For $T_e \geqslant$6000 K, it is interesting to note that a simplified 30-level model is accurate enough. Conversely, the 14-level model proposed by Kunc and Soon [6] appears to be unadapted to our whole temperature range.

3. Study of $\tau^C_{\rm QSS}$

In the preceding sections, we have pointed out that a three-body recombination rate coefficient exists only when the system is in a quasi-steady-state. Hence, before implementing this rate coefficient in flow codes, one has to check the validity of the QSS hypothesis [Eq. (12)]. The time-dependent approach used in this paper allows us to determine the relaxation time $\tau^C_{\rm QSS}$ necessary to reach a QSS starting at $t=0$ s from a given recombining situation.

For an optically thick case, Fig. 6 shows that $\tau^C_{\rm QSS}$ depends weakly on the electron temperature, but increases linearly with decreasing electron number density. We have also noticed a small influence on $\tau^C_{\rm QSS}$ by the initial distribution on the atomic levels for $T_e \geqslant$10 000 K, which is not represented in Fig. 6. For $n_e=10^{19}$ m^{-3}, the relaxation time $\tau^C_{\rm QSS}$ derived using Gryzinski's cross sections adapted to nitrogen [1] is also depicted. In this case, the elementary collisional rate coefficients are greater than or equal to those used in our model. As a consequence, the derived recombination rate k_r^C is higher (Fig. 4) and we note on Fig. 6 that the required relaxation time $\tau^C_{\rm QSS}$ is one order of magnitude shorter.

Finally, Fig. 6 shows that the three-body recombination rate k_r^C determined in this paper is adapted to study optically thick supersonic flows, where the characteristic flow time is about 10^{-6} s, only if $n_e \geqslant 10^{20}$ m^{-3}. For lower electron number densities or shorter flow times, it is necessary to consider one conservation equation for each atomic level i of the nitrogen atom.

4. Location of the critical level

In this study, we define the critical level p as the lowest atomic level at which the population N_p lies at the quasi-steady-state in the range of 10% above or below the Saha-Boltzmann value $N_P^{\rm SB}$. That is, for $t \geqslant \tau_{\rm QSS}$ and $q \geqslant p$ we have

$$0.9 \leqslant b(q) = N_q / N_q^{\rm SB} \leqslant 1.1. \tag{16}$$

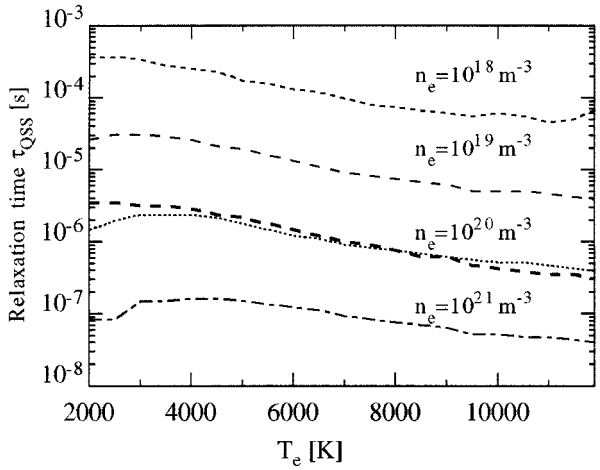

FIG. 6. Relaxation time $\tau^C_{\rm QSS}$ in an optically thick plasma. Thin lines correspond to different electron number densities. The thick dashed line represents the results obtained for $n_e=10^{19}$ m^{-3}, using the cross sections derived by Gryzinski and slightly modified to adapt nitrogen [1].

For an optically thick medium, we have noted that the critical level depends on the electron temperature, and not on either the initial distribution on the atomic levels or on the densities. Figure 7 shows that the number of levels in Saha-Boltzmann equilibrium increases with the electron temperature especially in the 2000–5000 K range. For $T_e \leqslant$2000 K, no atomic level is in equilibrium at the QSS. This result confirms that our atomic model does not allow us to determine k_r^C in this low temperature range (Fig. 5). Finally, for $T_e \geqslant$4500 K, it is interesting to note for practical applications that $p \leqslant 15$, and then all levels lying higher than 12.92 eV are in Saha-Boltzmann equilibrium.

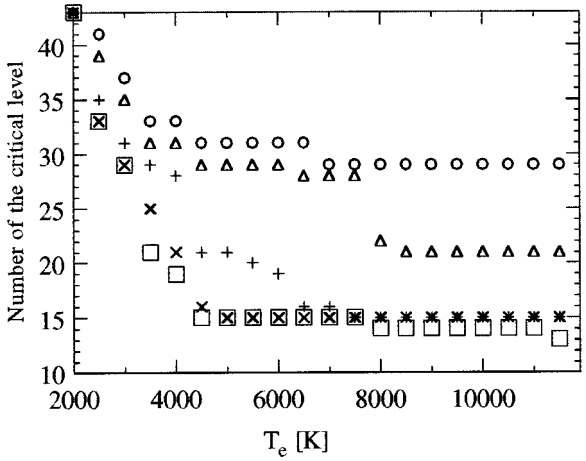

FIG. 7. Location of the critical atomic level. Square: optically thick case. Cross: $n_e=10^{21}$ m^{-3}; plus: $n_e=10^{20}$ m^{-3}; triangle: $n_e=10^{19}$ m^{-3}; and circle: $n_e=10^{18}$ m^{-3} in optically thin cases.

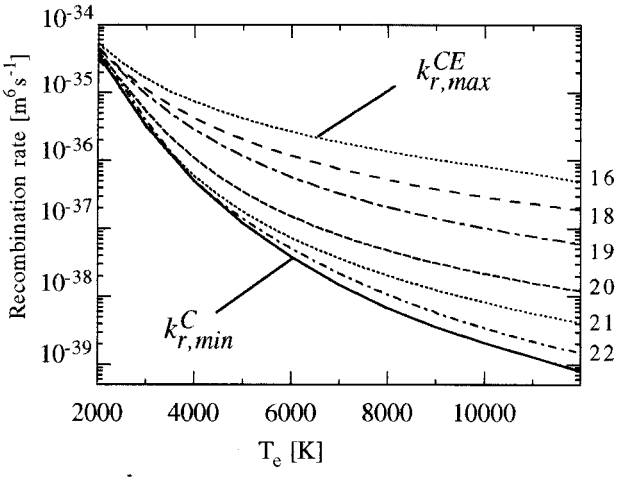

FIG. 8. Influence of spontaneous emission on the recombination rate in an optically thin plasma. Numbers at right denote x with $n_e = 10^x$ m^{-3}. For high electron number densities, the lower limit of the recombination rate, denoted $k^C_{r,\min}$, corresponds to the optically thick case value. For low electron number densities, the upper limit is denoted $k^{\mathrm{CE}}_{r,\max}$.

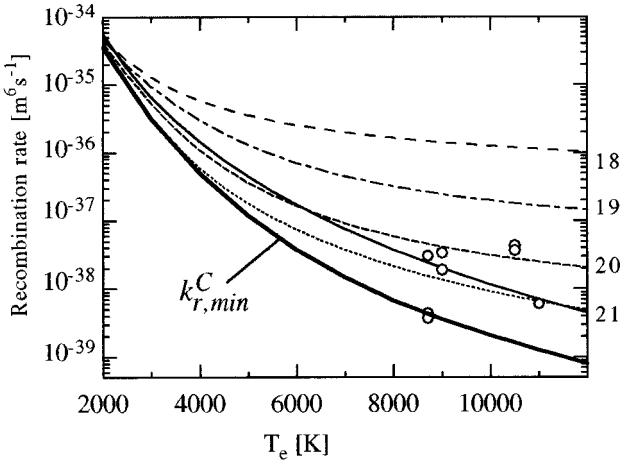

FIG. 9. Three-body recombination rate derived in taking into account all elementary processes, in an optically thin plasma. Numbers at right denote x with $n_e = 10^x$ m^{-3}. The thick solid line corresponds to the lower limit of the recombination rate for high electron number densities (optically thick case value). Circles correspond to experimental data [5]. The thin solid line is Park's fitting law [1].

D. Optically thin plasma

1. Determination of the effective three-body recombination rate coefficient

In an optically thin plasma, the results obtained for different initial recombining conditions indicate that the three-body recombination rate depends only on the electron temperature and the electron number density. First, if we neglect dielectronic and radiative recombination processes, Fig. 8 shows that the influence of spontaneous emission on the recombination rate (denoted, in this case, k_r^{CE}) decreases as either n_e increases or T_e decreases. As expected, for high electron number densities the recombination rate coefficient value converges to the lower limit obtained for an optically thick medium, denoted $k^{\mathrm{C}}_{r,\min}$ [Eq. (15)]. For electron number densities below 10^{16} m^{-3}, k_r^{CE} reaches an upper limit denoted $k^{\mathrm{CE}}_{r,\max}$. At low electron temperature, Fig. 8 confirms the importance of the highly excited (and nonradiating) levels on k_r^{CE}. Conversely, at high electron temperature, we note the influence of low energy and radiating atomic levels.

If we take into account all the elementary processes presented in Sec. III, Fig. 9 shows that, the lower the electron number density, the more dielectronic and radiative recombination processes increase the total recombination rate k_r. In this case, we have noted that k_r has no upper limit at low electron number density. These results are in qualitative agreement with those obtained earlier by Potapov *et al.* [3]. The comparison with Park's experimental data [5], which correspond to $n_e \approx 10^{21}$ m^{-3}, is rather satisfying if we take into account the uncertainty about escape factors and the overestimation of the experimental electron temperature [19]. It is also interesting to point out that Park's fitting law [1], initially derived for an optically thick plasma, corresponds with the results obtained with our model for an optically thin plasma where 10^{20} m$^{-3} \leqslant n_e \leqslant 10^{21}$ m^{-3} and 2000 K$\leqslant T_e \leqslant$12 000 K.

When all elementary processes are considered, the contribution of radiative and dielectronic recombinations can be easily isolated in the general Eq. (11). Then this equation can be simply written as

$$\frac{dn_e}{dt} = \dot{n}_e = k_i n_e N_a - k_r^{\mathrm{CF}} n_e^3 - \alpha^R n_e^2 \tag{17}$$

where k_r^{CE} takes into account all the elementary collisional processes and spontaneous emission (Fig. 8), and α^R takes into account dielectronic and radiative recombination processes. The total recombination rate k_r is therefore $k_r^{\mathrm{CE}} + \alpha^R/n_e$. This formulation is of great interest, since in the present work α^R has been expressed analytically. For an optically thin plasma, we have

$$\alpha^R = \sum_{i=1}^{3} [\alpha_i^{\mathrm{RR}} + \alpha_i^{\mathrm{RD}}] = \alpha^{\mathrm{RR}} + \alpha^{\mathrm{RD}}, \tag{18}$$

where α^{RR} and α^{RD} are given by Eqs. (8) and (9).

We have also fitted k_r^{CE} (Fig. 8) for different electron number densities to the following expression:

$$k_r^{\mathrm{CE}} = A T_e^b \ \mathrm{m^6\,s^{-1}}, \quad 2000\ \mathrm{K} \leqslant T_e \leqslant 12\,000\ \mathrm{K}. \tag{19}$$

The coefficients A and b are given in Table II. The dis-

TABLE II. Parameters in the effective three-body recombination rate coefficient k_r^{CE} for different electron number densities.

n_e (m^{-3})	A (m^6 s^{-1} K^{-b})	b
10^{18}	6.29×10^{-25}	-3.09
10^{19}	4.37×10^{-23}	-3.66
10^{20}	1.03×10^{-20}	-4.42
10^{21}	3.05×10^{-19}	-4.89

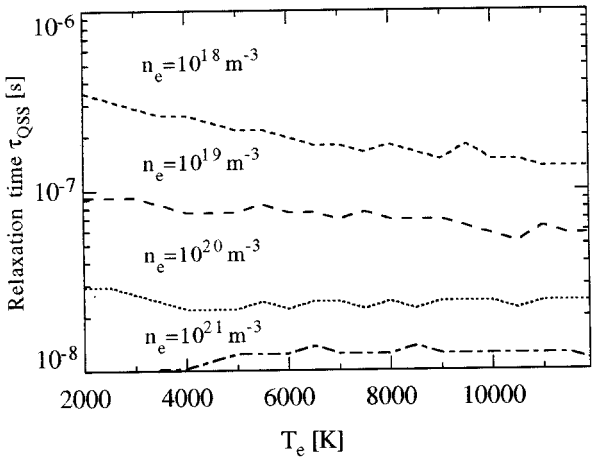

FIG. 10. Relaxation time τ_{QSS} in an optically thin plasma for different electron number densities.

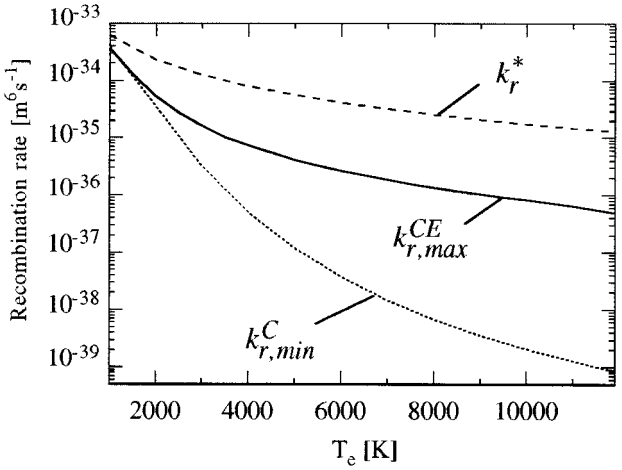

FIG. 11. Different definitions of the three-body recombination coefficient k_r^{CE}. k_r^* is the one-way coefficient and $k_{r,\mathrm{min}}^{C}$ and $k_{r,\mathrm{max}}^{\mathrm{CE}}$ are defined in Fig. 8.

crepancy between the total recombination rate value calculated with the analytical expressions [Eqs. (8), (9), and (19)], and the one determined directly and represented in Fig. 9, remains within a factor of 2.

2. Study of τ_{QSS}

In an optically thin plasma, Fig. 10 shows that the required relaxation time τ_{QSS} depends on n_e and T_e as in an optically thick plasma. However, radiative processes enhance recombination, and then the required τ_{QSS} is significantly shorter in an optically thin case than in an optically thick medium. That is, for $n_e=10^{19}$ m^{-3}, the discrepancy is about two orders of magnitude. Finally, Fig. 10 indicates that in the computation of an optically thin supersonic nitrogen plasma flow, where the characteristic flow time is about 10^{-6} s and the electron number density exceeds 10^{18} m^{-3}, the recombination rate coefficient k_r derived in this paper can be used. For lower electron number densities or shorter flow times, it is necessary to consider one conservation equation for each atomic level i of the nitrogen atom.

3. Location of the critical level

When radiative processes are taken into account, Fig. 7 shows that the critical level p decreases as T_e and n_e increase. For a high electron number density, the critical level converges to the one obtained for an optically thick medium. This result puts forward that, for a given electron number density, the reabsorption of the emitted radiation tends to increase the number of levels in equilibrium with the continuum. For practical applications, it is interesting to note that, for $n_e \geqslant 10^{19}$ m^{-3} and $T_e \geqslant 4500$ K, the critical level p is lower or equal to 14; then all atomic levels lying higher than 14 eV are in Saha-Boltzmann equilibrium.

E. Comments on the definition of k_r

Following the method described above to determine α^R, one could propose to derive an expression for the effective three-body recombination rate coefficient directly from Eq. (11):

$$k_r^* = \sum_i \beta_{ci}(T_e) = f(T_e). \tag{20}$$

This coefficient takes into account only direct recombination processes on the atomic levels, and neglects the other processes which link the atomic level populations together. Figure 11 compares this coefficient k_r^* with $k_{r,\mathrm{min}}^{C}$ and $k_{r,\mathrm{max}}^{\mathrm{CE}}$ defined in the preceding sections. The smallest discrepancy between the three different values is obtained for $T_e < 2000$ K. This result confirms the importance of direct recombination processes on highly excited levels in the low electron temperature range. When the electron temperature increases, k_r^* remains higher than $k_{r,\mathrm{max}}^{\mathrm{CE}}$ (one order of magnitude difference at 12 000 K). In conclusion, k_r^* is a mathematical coefficient with no physical interest to describe the $N^+ + 2e^- \rightarrow N + e^-$ global recombination process. This result already mentioned by Park [1] is clearly illustrated in this paper. In fact, the present work confirms the importance of taking into account the quasi-steady-state condition to derive a meaningful recombination coefficient.

F. Determination of the effective ionization rate coefficient

In order to introduce the general Eq. (17) in flow codes, we also have to determine the effective ionization rate coefficient k_i. In fact, the general method described in the preceding sections to derive the effective recombination rate coefficient can be used. That is, starting at $t=0s$ from an ionizing situation, the value of the ionization coefficient is given by the value of the ratio $\dot{n}_e/(n_e N_a)$ [Eq. (17)] at the quasi-steady-state. However, it is interesting to point out that ionization and recombination rate coefficients are not independent. Indeed, at the stationary state of the reaction $N^+ + 2e^- \leftrightarrow N + e^-$ the terms on the right-hand side of Eq. (17) have to balance to give $\dot{n}_e = 0$. In the optically thick case, we simply have

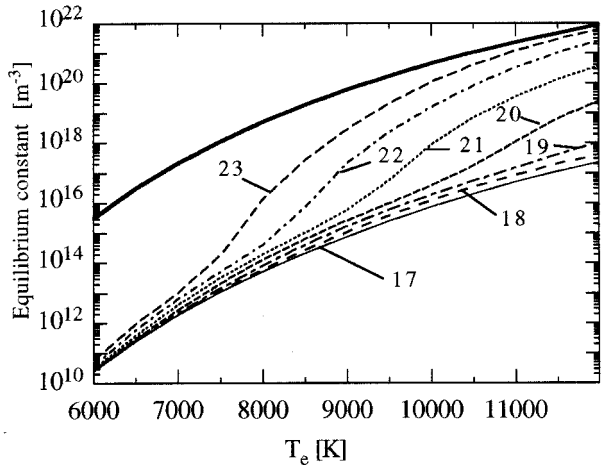

FIG. 12. Influence of spontaneous emission on the equilibrium constant in an optically thin plasma. Numbers denote x with $N_t = 10^x$ m^{-3}. The thick solid line corresponds to the Saha value.

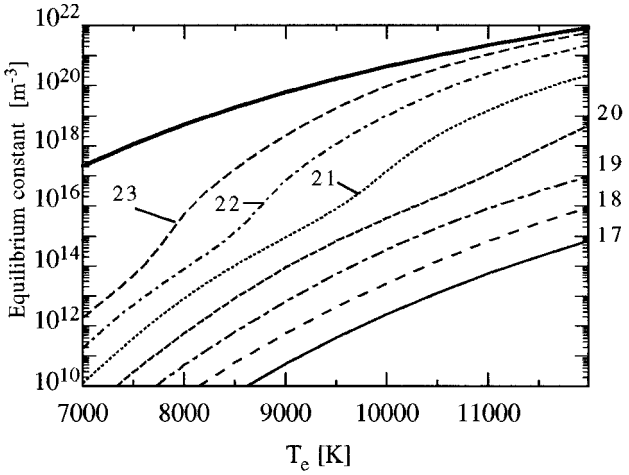

FIG. 13. Equilibrium constant derived in taking into account all elementary processes in an optically thin plasma. Numbers denote x with $N_t = 10^x$ m^{-3}. The thick solid line corresponds to the Saha value.

$$k_i^C = k_r^C \frac{[n_e^{\mathrm{Stat}}]^2}{N_a^{\mathrm{Stat}}} = k_r^C K^{\mathrm{Stat}} = k_r^C K^{\mathrm{Saha}}(T_e). \qquad (21)$$

In this case, the stationary state corresponds to a Saha equilibrium at the electron temperature T_e, and consequently k_i^C is only a function of T_e. In an optically thin plasma, radiative processes enhance recombination and, then, the ionization degree at the stationary state is lower than the one corresponding to the Saha equilibrium. Consequently, $K^{\mathrm{Stat}} < K^{\mathrm{Saha}}$, where K^{Stat} depends on T_e but also on densities. As Kunc and Soon [6] clearly explained it, the most characteristic density of the nonequilibrium properties of the stationary state is the total particle density N_t [6] (note that the definition of N_t proposed by these authors is the double of ours) and not the electron number density usually used [3]. First, neglecting radiative and dielectronic recombinations, Fig. 12 depicts the equilibrium constant as a function of T_e for different values of N_t. The discrepancy with the Saha value is significant, especially at low electron temperatures. When electron temperature and densities increase, collisional processes become more efficient than radiative processes, and then the equilibrium constant values are closer to those corresponding to a Saha equilibrium.

Figure 13 shows that the lower limit of the equilibrium constant for low densities disappears when radiative and dielectronic recombination processes are taken into account. In their work, Kunc and Soon [6] studied more precisely the reabsorption of the emitted radiation, but neglected a few transitions that we have considered in our model. Therefore a direct comparison of their computed densities at the stationary state with ours cannot be made; however, a qualitative agreement is observed. Finally, this study clearly shows that, with the nonlinear dependence of K^{Stat} on N_t, and the uncertainty on escape factors, it turns out to be very difficult to derive handy analytical expressions for k_i to be implemented in flow codes. However, data files giving K^{Stat} as a function of T_e for different values of N_t can be obtained from the authors.

VI. CONCLUSIONS

In this paper, we have studied the effective three-body recombination rate coefficient of nitrogen in a plasma where 10^{18} m$^{-3} \leqslant n_e \leqslant 10^{21}$ m^{-3} and 2000 K$\leqslant T_e \leqslant$12 000 K. In the optically thick case, we propose an analytical expression of the recombination coefficient to be implemented in flow codes:

$$k_r^C = 1.96 \times 10^{-39} \left(\frac{T_e}{10^4} \right)^{-6.04} \ \mathrm{m^6\ s^{-1}}$$

$$\text{for } 2000\ \mathrm{K} \leqslant T_e \leqslant 12\,000\ \mathrm{K}. \qquad (15)$$

This rate coefficient value remains smaller than the one given by Park's fitting law [1], and the discrepancy exceeds one order of magnitude for $T_e > 8000$ K. In an optically thin plasma, radiative processes enhance recombination and then increase the effective recombination coefficient, especially at high electron temperatures. In this paper, we have taken into account the dielectronic recombination process which is usually neglected, but turns out to be more efficient than the radiative recombination process at electron temperatures below 20 000 K. Finally, we have shown that the effective three-body recombination rate coefficient k_r could be written as $k_r^{\mathrm{CE}} + \alpha^R / n_e$, where k_r^{CE} takes into account all the elementary collisional processes and spontaneous emission and α^R dielectronic and radiative recombination processes. In order to implement these new results easily in flow codes, we propose simple analytical expressions for k_r^{CE} [see Eq. (19) and Table II] and α^R [see Eqs. (8) and (9)]. It is interesting to point out that Park's fitting law, which has been established in using inaccurate collision cross sections in an optically thick medium, turns out to correspond with the recombination coefficient derived in this paper for an optically thin plasma where 10^{20} m$^{-3} \leqslant n_e \leqslant 10^{21}$ m^{-3} and 2000 K$\leqslant T_e \leqslant$12 000 K.

The associated effective ionization rate coefficient k_i has been determined in taking into account that effective ionization and recombination coefficients are related by the stationary state of the reaction $N^+ + 2e^- \leftrightarrow N + e^-$. In the optically thick case, the stationary state is a Saha-Boltzmann equilibrium, and the equilibrium constant depends only on T_e. In the optically thin case, the equilibrium constant value is lower, and depends on T_e and the total density N_t.

This study has once more confirmed the importance of the quasi-steady-state (QSS) condition to determine meaningful rate coefficients. A time-dependent approach has allowed us to study the relaxation time τ_{QSS} necessary to reach a QSS, which limits the validity of the derived rate coefficients. For recombining plasmas, we have pointed out that τ_{QSS} depends on T_e and n_e. At a given electron number density the longest relaxation time corresponds to an optically thick medium. Then the effective three-body recombination rate coefficient derived in this paper may be implemented in the computation of supersonic plasma flows, where the characteristic flow time is about 10^{-6} s, for an electron number density higher than 10^{18} m^{-3} if the plasma is optically thin, and for electron number density higher the 10^{20} m^{-3} if the plasma is optically thick. For lower densities or shorter flow times, it is necessary to compute one conservation equation for each atomic level i of the nitrogen atom.

For experimental applications, we have also studied the location of the lowest atomic level which population is in Saha-Boltzmann equilibrium at the quasi-steady-state. We have shown that the number of atomic levels in Saha-Boltzmann equilibrium increases with n_e and T_e. For $T_e \geqslant 4500$ K, in an optically thick plasma and in an optically thin plasma with $n_e \geqslant 10^{19}$ m^{-3}, all levels lying higher than 12.9 and 14 eV, respectively, are in Saha-Boltzmann equilibrium.

The accuracy of the final results of this work depends on the choice of the atomic model and on the accuracies of the cross sections and Einstein coefficients. First, we have shown that the accuracy of highly excited level population determinations limits at low electron temperatures the accuracy of the derived recombination coefficient. In order to study electron temperatures below 2000 K, it would be necessary to consider a more detailed atomic model for highly excited levels than the one used in this paper. Second, we have pointed out that k_r and τ_{QSS} values depend significantly on the choice of the cross sections for electron-impact excitation and deexcitation processes. We consider that the Vainshtein formalism [21] is certainly more adapted to determine these cross sections for low atomic levels than hydrogenic models used in earlier studies [1]. However, it is important to note that the Vainshtein approach is based on a Born approximation. Currently, more accurate quantum mechanical methods such as close-coupling and R-matrix methods are available, but they are computer time intensive and have been completed only for a few systems [35].

In this work, the treatment of radiation has been reduced to the two limits of optically thick and optically thin cases. It would be interesting to develop the modeling of radiation escape factors in order to study more precisely the influence of the reabsorption of radiation on the results. However, it should be pointed out that these effects will not change the general characteristics of the results discussed in this paper.

[1] C. Park, AIAA J. **7**, 1653 (1969).
[2] J. L. Kulander, J. Quantum Spectrosc. Radiat. Transfer **5**, 253 (1965).
[3] A. V. Potapov, L. E. Tsvetkova, V. I. Antropov, and G. N. Volkova, Opt. Spektrosk. **43**, 412 (1977) [Opt. Spectrosc. (USSR) **43**, 243 (1977)].
[4] R. D. Taylor and A. W. Ali, J. Quantum Spectrosc. Radiat. Transfer **35**, 213 (1986).
[5] C. Park, AIAA J. **6**, 2090 (1968).
[6] J. A. Kunc and W. H. Soon, Phys. Rev. A **40**, 5822 (1989).
[7] C. A. Ramsbottom and K. L. Bell, Phys. Scr, **50**, 666 (1994).
[8] J. R. Fuhr and W. L. Wiese, *Atomic Transition Probabilities*, edited by D. R. Lide, CRC Handbook of Chemistry and Physics (CRC Press, Boca Raton, FL, 1990), pp. 128–179.
[9] A. Hibbert, E. Biémont, M. Godefroid, and N. Vaeck, Astron. Astrophys. Suppl. Ser. **88**, 505 (1991).
[10] C. Goldbach, T. Lüdtke, M. Martin, and G. Nollez, Astron. Astrophys. **266**, 605 (1992).
[11] M. Cacciatore, M. Capitelli, and H. W. Drawin, Physica **84C**, 267 (1976).
[12] K. Sawada and T. Fujimoto, Phys. Rev. E **49**, 5565 (1994).
[13] C. C. Limbaugh and A. A. Mason, Phys. Rev. A **4**, 2368 (1971).
[14] M. Cacciatore and M. Capitelli, J. Quantum Spectrosc. Radiat. Transfer **16**, 325 (1976).
[15] H. R. Griem, *Plasma Spectroscopy* (McGraw-Hill, New-York, 1964).
[16] A. Unsöld, Z. Astrophys. **24**, 355 (1948).
[17] H. N. Olsen, J. Quantum Spectrosc. Radiat. Transfer **3**, 305 (1963).
[18] C. Park, J. Quantum Spectrosc. Radiat. Transfer **8**, 1633 (1968).
[19] C. Park, J. Plasma Phys. **9**, 187 (1973).
[20] C. Park, *Non-Equilibrium Hypersonic Aerothermodynamics* (Wiley, New York, 1990).
[21] I. I. Sobelman, L. A. Vainshtein, and E. A. Yukov, *Excitation of Atoms and Broadening of Spectral Lines* (Springer-Verlag, New York, 1981).
[22] M. Gryzinski, Phys. Rev. A **138**, 322 (1965).
[23] C. Park, J. Quantum Spectrosc. Radiat. Transfer **11**, 7 (1971).
[24] R. J. Henry, P. G. Burke, and A. L. Sinfailam, Phys. Rev. **178**, 218 (1969).
[25] H. W. Drawin, Report No. EUR-CEA-FC-383, Fontenay-aux-Roses, France, 1967 (unpublished).
[26] M. Gryzinski and J. A. Kunc, J. Phys. B **19**, 2479 (1986).
[27] C. Goldbach, M. Martin, G. Nollez, P. Plomdeur, J. P. Zimmermann, and D. Babic, Astron. Astrophys. **161**, 47 (1986).
[28] C. Goldbach and G. Nollez, Astron. Astrophys. **201**, 189 (1988).
[29] H. Nussbaumer and P. J. Storey, Astron. Astrophys. **126**, 75 (1983).

[30] H. Nussbaumer and P. J. Storey, Astron. Astrophys. Suppl. Ser. **56**, 293 (1984).
[31] R. J. Henry, Astrophys. J. **161**, 1153 (1970).
[32] A. C. Hindmarsh, ACM SIGNUM Newslett. **15** (1980).
[33] P. Domingo, A. Bourdon, and P. Vervisch, Phys. Plasmas **2**, 2853 (1995).
[34] D. R. Bates, A. E. Kingston, and R. W. P. McWhirter, Proc. R. Soc. London **267**, 297 (1962).
[35] A. K. Pradhan, in *Atomic Processes in Plasmas*, edited by A. Hauer and A. L. Mertf (Academic, New York, 1988).